

Article

# Fabrication of Biocompatible Polycaprolactone–Hydroxyapatite Composite Filaments for the FDM 3D Printing of Bone Scaffolds

Chang Geun Kim <sup>1,†</sup>, Kyung Seok Han <sup>1,†</sup>, Sol Lee <sup>1</sup>, Min Cheol Kim <sup>1</sup> , Soo Young Kim <sup>2,\*</sup> and Junghyo Nah <sup>1,\*</sup> 

<sup>1</sup> Department of Electrical Engineering, Chungnam National University, Daejeon 34134, Korea; cgkim@o.cnu.ac.kr (C.G.K.); ynwahan@cnu.ac.kr (K.S.H.); lee\_sol@cnu.ac.kr (S.L.); mcheol1@o.cnu.ac.kr (M.C.K.)

<sup>2</sup> College of Pharmacy, Yeungnam University, Gyeongsan-si 38541, Korea

\* Correspondence: sooykim@yu.ac.kr (S.Y.K.); jnah@cnu.ac.kr (J.N.)

† These authors equally contributed.

**Abstract:** Recently, three-dimensional printing (3DP) technology has been widely adopted in biology and biomedical applications, thanks to its capacity to readily construct complex 3D features. Using hot-melt extrusion 3DP, scaffolds for bone tissue engineering were fabricated using a composite of biodegradable polycaprolactone (PCL) and hydroxyapatite (HA). However, there are hardly any published reports on the application of the fused deposition modeling (FDM) method using feed filaments, which is the most common 3D printing method. In this study, we report on the fabrication and characterization of biocompatible filaments made of polycaprolactone (PCL)/hydroxyapatite (HA), a raw material mainly used for bone scaffolds, using FDM 3D printing. A series of filaments with varying HA content, from 5 to 25 wt.%, were fabricated. The mechanical and electrical properties of the various structures, printed using a commercially available 3D printer, were examined. Specifically, mechanical tensile tests were performed on the 3D-printed filaments and specimens. In addition, the electrical dielectric properties of the 3D-printed structures were investigated. Our method facilitates the fabrication of biocompatible structures using FDM-type 3DP, creating not only bone scaffolds but also testbeds for mimicking bone structure that may be useful in various fields of study.

**Keywords:** fused deposition modeling 3D printing; bone scaffold; 3D printing filaments; hydroxyapatite and polycaprolactone composite



**Citation:** Kim, C.G.; Han, K.S.; Lee, S.; Kim, M.C.; Kim, S.Y.; Nah, J. Fabrication of Biocompatible Polycaprolactone–Hydroxyapatite Composite Filaments for the FDM 3D Printing of Bone Scaffolds. *Appl. Sci.* **2021**, *11*, 6351. <https://doi.org/10.3390/app11146351>

Academic Editor: Anming Hu

Received: 1 June 2021

Accepted: 7 July 2021

Published: 9 July 2021

**Publisher's Note:** MDPI stays neutral with regard to jurisdictional claims in published maps and institutional affiliations.



**Copyright:** © 2021 by the authors. Licensee MDPI, Basel, Switzerland. This article is an open access article distributed under the terms and conditions of the Creative Commons Attribution (CC BY) license (<https://creativecommons.org/licenses/by/4.0/>).

## 1. Introduction

Additive manufacturing (AM), also referred to as 3D printing (3DP), is a technology that is used to fabricate complex structures from 3D model data [1]. For this reason, 3D printing has been widely used in various fields, including machinery, architecture, automobiles, and electronics [1–3]. In recent years, the 3DP of biomaterials or biocompatible materials has been actively investigated, including in biology and biomedical applications [4–6]. Accordingly, various biomaterials or biocompatible materials that are suitable for 3D printing have been developed [7,8]. For printing these biocompatible materials or biomaterials, several types of 3D printer have been used, such as fused deposition modeling (FDM), stereolithography (SLA), and digital light processing (DLP). However, there is a limited choice of biocompatible materials available for 3DP, and it is even more difficult to find suitable materials for FDM 3D printing, the most widely used 3D printing method. Thus, development of biocompatible 3DP filament for FDM 3D printers can promote and expand the application of FDM 3DP for bioengineering and biomedical research. Specifically, this method can be useful for the preparation of personalized bone scaffolds and artificial bone testbeds.

Used in tissue engineering, a bone scaffold promotes bone cell migration, which is important for vascularization and bone in-growth, and also provides temporary mechanical support to fractured or injured sites [9,10]. To be adoptable as a bone scaffold, however, the material must be self-degradable without producing toxic byproducts [9]. For bone scaffold fabrication, composites of hydroxyapatite (HA) and polycaprolactone (PCL) have been widely used. HA has a similar composition to native bone and has been used in various biomedical applications, for example, as a bone scaffold, as a filler, as an implant coating and as a drug delivery system, due to its osteoconductive and biocompatible properties [11–13]. HA is an essential material for bone scaffolds, as it shares 70% of the native bone's composition; however, its brittle nature limits its use as a scaffold [12,13]. PCL is also a widely used biocompatible and biodegradable polymer [13], which makes it similarly suitable for various biomedical applications, such as bone scaffolds or long-term implantable drug delivery systems. [14]. Thus, PCL is generally used together with HA to provide the appropriate mechanical strength required for a scaffold [13,15,16]. For the fabrication of bone scaffolds using a PCL/HA composite, various fabrication methods, such as salt leaching [13], thermally induced phase-separation (TIPS) [15], and 3D printing [17,18] have been employed. Briefly, salt leaching is a method of fabricating a porous structure by pouring composites mixed with NaCl particles into a mold to make a shape, then rinsing it in water to remove the NaCl. The TIPS process is a method of removing the solvent by freezing the composite solution into a gel and soaking it in excess cold water. Both methods are suitable for fabricating well-defined porous structures, but it is difficult to readily create customized structures. Among these fabrication methods, 3D printing is the best at facilitating the formation of complex structures, as well as customized scaffold preparation. Thus, several 3D-printed scaffolds have been reported over the years [11,16,19–27]. However, the aforementioned FDM (fused deposition modeling) 3DP method is rarely used to fabricate scaffolds, even though it offers several advantages over other 3DP methods, such as versatility, convenience, and accessibility [4,5]. It is because there are no PCL/HA composite filaments available for FDM 3DP, to the best of our knowledge.

In this work, we report on the fabrication of PCL/HA composite filaments for FDM 3DP and demonstrate the mechanical and electrical properties of the filaments and the printed specimens. Specifically, filaments with a varying HA contents of 5, 10, 15, 20, and 25 wt.% were produced, and the mechanical properties of these filaments, as well as the 3D-printed specimens produced with them, were evaluated. In addition, the dielectric constant of various PCL/HA composites—a parameter not previously reported on in the literature—was also measured, in order to assess the potential application of this material as a bone mimetic testbed for implantable wireless devices. Lastly, using the composite filaments developed in this work, bone scaffolds and mimetic bones were fabricated using a typical FDM 3D printer.

## 2. Materials and Methods

### 2.1. Materials

PCL and HA nanopowder were purchased from Sigma-Aldrich (Sigma-Aldrich: St. Louis, MO, USA), and N,N-Dimethylformamide (DMF) was purchased from Daejung.

### 2.2. Methods

#### 2.2.1. Fabrication of PCL/HA Composite Filaments

The process of synthesizing PCL/HA composite flakes is displayed in Figure 1. First, separate solutions of PCL and HA dissolved in DMF were prepared, and stirred overnight at 100 °C. During the stirring process, the beakers containing both solutions were sealed with aluminum foil to prevent evaporation of the DMF solvent. Next, both solutions were mixed in the same container, then stirred for 60 min, before being ultrasonicated in a sonication bath for 30 min. Following this, the PCL/HA composite solution was divided into small containers. To evaporate the DMF from the solution, the container was heated to

100 °C and the solution was stirred until the DMF had completely evaporated. Once the PCL/HA composite solution had solidified, the container was sonicated to separate the solidified flakes from the beakers. Lastly, the PCL/HA composite was cut into small pieces and dried at room temperature.

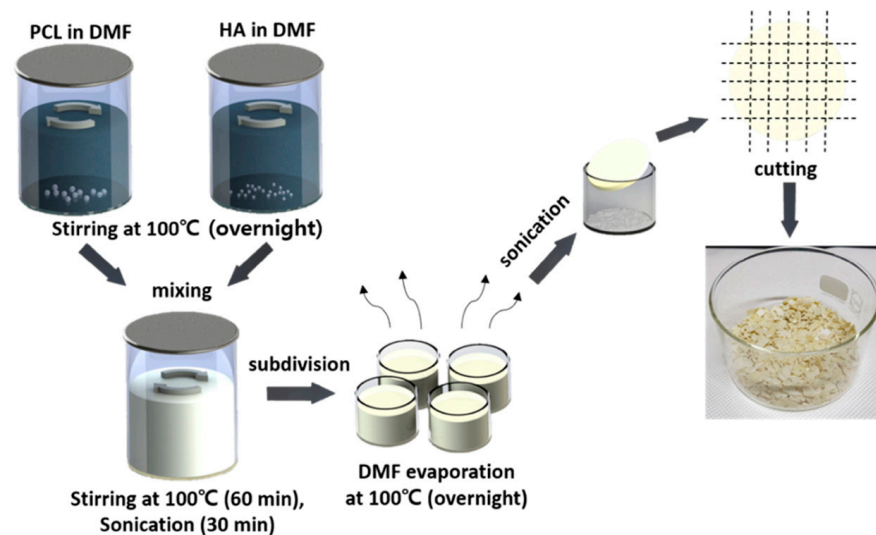


**Figure 1.** Schematic of the PCL/HA composite flake preparation steps. Photograph showing the PCL/HA composite flakes after evaporating the solvent from the composite solution.

Using the synthesized PCL/HA composite flakes, 3D FDM filaments were fabricated using a Filabot EX2 extruder with a 1.75 mm extrusion nozzle, as shown in Figure 2. Instead of air cooling the extruded filaments, we used a water bath to rapidly cool them down, thus minimizing thermal deformation. The composite flakes loaded in the extruder were extruded as a PCL/HA composite filament, and the extruded filament was guided to a drive wheel, which was then wound at a constant speed. All the filaments of varying composition were extruded at 100 °C, and the dial speed of extrusion and spooler was adjusted until the diameter of the filaments became uniform.

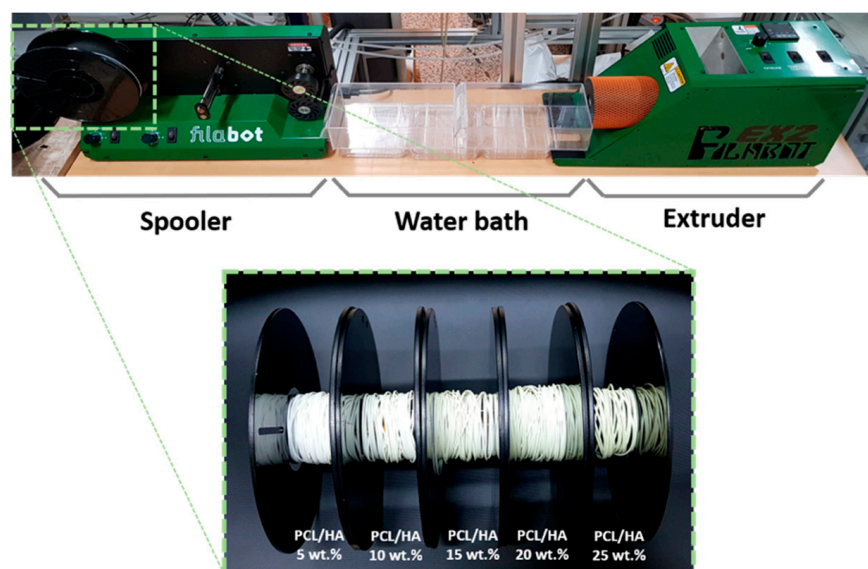


**Figure 2.** Photographs of Filabot EX2, consisting of spooler, water bath, and extruder (top). Fabricated filaments with various HA wt.% produced using the above filament extruder (bottom).

The morphology of the extruded filaments was evaluated, using a scanning electron microscope (SEM) to identify whether filaments had been fabricated without voids, which can greatly affect the quality of the 3D printout. Before loading into the SEM, the filaments were Pt-sputtered and observed at 10 keV. Filaments of varying composition were cut into 8 cm pieces for tensile testing using a custom-built bending machine. The stress was recorded at steps of 0.5 mm.

### 2.2.2. 3D-Printed Films Using Fabricated PCL/HA Composite Filaments

To print 3D specimens from the fabricated filaments, they were fed into a 3D printer (Dr. InVivo 4D2, ROKIT Healthcare: Seoul, Korea) with a 0.4 mm nozzle. The 3D printer settings were optimized for each filament. All the filaments used in this work were printed at a printing temperature of 130 °C, a bed temperature of 30 °C, a fill density of 100%, a layer height of 0.1 mm, an infill rotation angle of 90°, and a travel speed of 10 mm/s. However, the input flow was different for each composite filament (Table 1). X-ray diffraction (XRD) analysis was conducted to identify the XRD pattern of the PCL/HA composites. The specimens for XRD analysis were printed to the dimensions of 20 mm(L) × 20 mm(W) × 2 mm(T). The tensile tests were performed using 3D-printed specimens with dimensions of 30 mm(L) × 5 mm(W) × 0.5 mm(T). The stress vs. strain was recorded at 0.5 mm steps. The dielectric constant was measured by varying the HA content and specimens for this were prepared with dimensions of 15 mm(L) × 15 mm(W) × 5 mm(T).

**Table 1.** 3D printing settings for each PCL/HA filament.

PCL/HA Composite	Temperature [°C]	Input Flow [%]
PCL/HA 5 wt.%	130	175
PCL/HA 10 wt.%	130	140
PCL/HA 15 wt.%	130	110
PCL/HA 20 wt.%	130	150
PCL/HA 25 wt.%	130	130

## 3. Results and Discussion

### 3.1. Morphology of PCL/HA Composite Filaments

Figure 3 shows the cross-sectional SEM images of the fabricated filaments with different HA wt.%. As noted, voids in the filament can cause malfunctions during the extrusion process, resulting in porous and deformed 3D printouts. In the inset images, a circular shape was observed in the cross-section of all filaments, without any notable deformation. In addition, we examined the cross-section of multiple samples of each filament and did not observe any voids in the filament structure. Therefore, all the fabricated filaments were suitable for FDM 3D printing. However, a slightly rough surface with a root mean square average height of 162 nm, as measured by atomic force microscopy, was observed on the surface of the cross-section of the filament with 25 wt.% HA, in contrast with the filaments with a lower HA content.

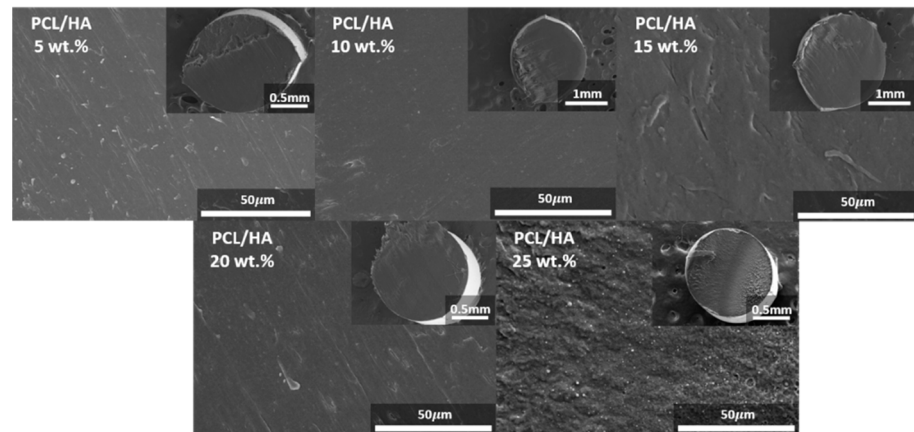


**Figure 3.** Cross-sectional SEM images of the fabricated filaments containing various HA wt.%. The insets show the overall shapes of the filaments at a low magnification.

### 3.2. XRD Characterization

The phase of the PCL/HA composite filaments was analyzed by means of XRD, as shown in Figure 4. HA exhibited weak intensity peaks, due to its relatively poor crystallinity [13], but the observed intensity peaks still corresponded to the characteristic peaks of HA. On the other hand, relatively strong intensity peaks were observed in PCL, compared to HA, due to its semi-crystalline nature. PCL exhibits two strong diffraction peaks at Bragg angles  $2\theta = 21.3^\circ$  and  $23.6^\circ$  [28], and our peaks demonstrated the same result. Thus, in the XRD patterns of the PCL/HA composites, both characteristic peaks can be clearly observed. However, it can be seen that as the wt.% of HA in the PCL/HA composite increased, the intensity peaks corresponding to PCL decreased. Therefore, the XRD analysis indicates that the PCL/HA composite filaments were correctly synthesized and there was no change in their properties during the filament fabrication and 3D printing processes.

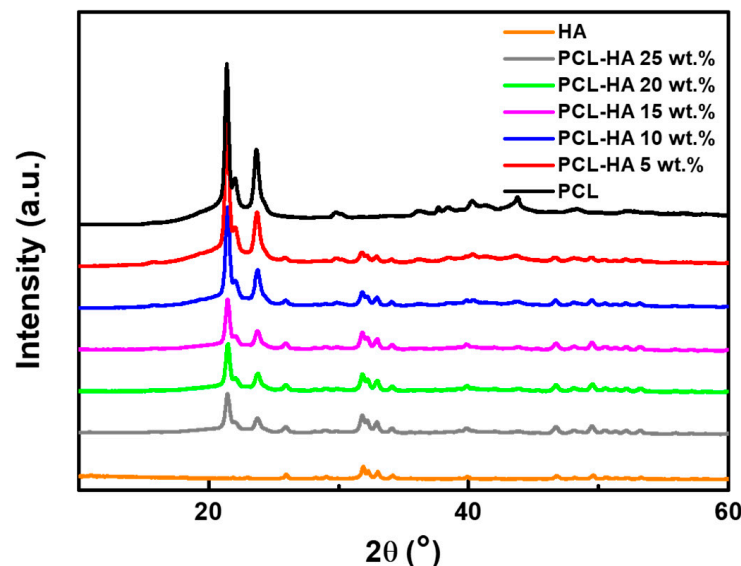


**Figure 4.** XRD patterns of the PCL/HA composites. Characteristic peaks corresponding to HA and PCL can both be observed in the PCL/HA composite filaments.

### 3.3. Mechanical Properties of PCL/HA Composite Filaments and 3D-Printed Films

Figure 5a shows the tensile stress–strain curves of the fabricated composite filaments. As noted, HA has poor mechanical properties, and both tensile strength and fracture strain decrease as the HA content in the composite filament increases. A PCL/HA composite filament with 30 wt.% HA was also fabricated, but was too brittle to be used as a filament.

Indeed, the PCL/HA composite filament with 30 wt.% HA displayed a drastic reduction in tensile strength and fracture strain. Thus, the 30 wt.% HA composite was excluded from the potential filament options covered in this work. The mechanical properties of the variously composed PCL/HA composite filaments are summarized in Table 2.

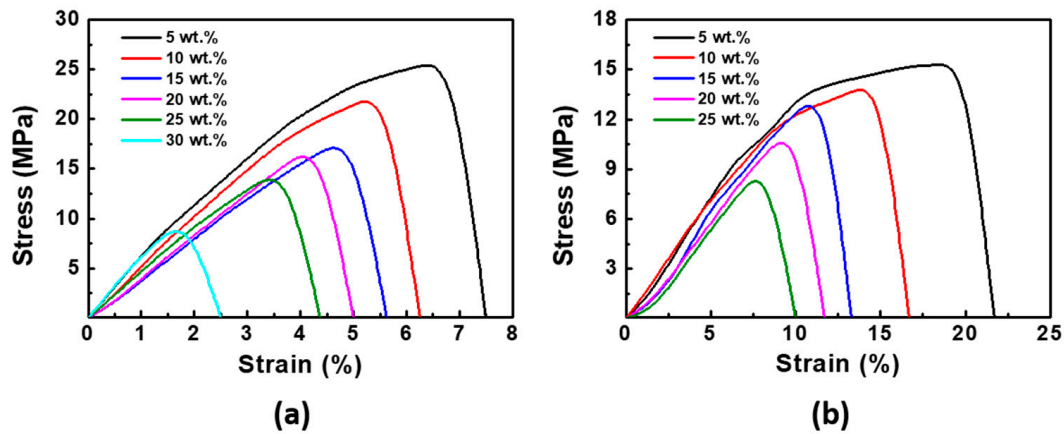


Figure 5. Tensile stress–strain curve of (a) fabricated filaments. (b) 3D-printed specimen.

Table 2. Mechanical properties of the PCL/HA composite filaments and 3D-printed PCL/HA composite thin films.

PCL/HA Composite	Filament		Thin Film	
	Tensile Strength (MPa)	Fracture Strain (%)	Tensile Strength (MPa)	Fracture Strain (%)
PCL/HA 5 wt.%	25.91	7.5	15.40	21.7
PCL/HA 10 wt.%	22.90	6.3	14.31	16.7
PCL/HA 15 wt.%	18.24	5.6	13.83	13.3
PCL/HA 20 wt.%	17.67	5.0	11.69	11.7
PCL/HA 25 wt.%	15.15	4.4	9.44	10.0
PCL/HA 30 wt.%	10.25	2.5	-	-

Next, using the prepared filaments with HA contents of 5 to 25 wt.%, thin films with a thickness of 0.5 mm were printed for testing. Figure 5b shows the stress–strain curves of the 3D-printed thin films; the results are consistent with those observed from the tests with the filaments. It can be noted that curves of the PCL/HA composite filaments with a 5 and 10 wt.% HA content are non-linear, which is attributable to the ductile nature of PCL. The mechanical properties of 3D-printed thin films are summarized in Table 2.

### 3.4. Electrical Properties

Recently, bone-implantable wireless devices have been actively investigated [29,30]. Bone mimetic platforms are necessary for evaluating the performance of such devices. PCL/HA composite filaments can be potentially used to build such platforms, and the dielectric properties of the composite structure is one of the key parameters that must be known. However, the dielectric properties of PCL/HA composite structures have yet to be reported. To find the dielectric constants and losses in structures fabricated with PCL/HA composite filaments, structures with dimensions of 15 mm(L) × 15 mm(W) × 5 mm(T) were printed. Each structure was printed with 100% filling density, because a porous structure may reduce the dielectric constant. Figure 6a shows the measured dielectric constants of the PCL/HA composite structures with varying HA content. As the wt.% of HA increased, the dielectric constant of each structure increased proportionally, although difference was not significant in the measurement frequency, since the molecules in the structure cannot respond to frequency changes in the GHz range. The dielectric loss was small, close to zero, as shown in Figure 6b.

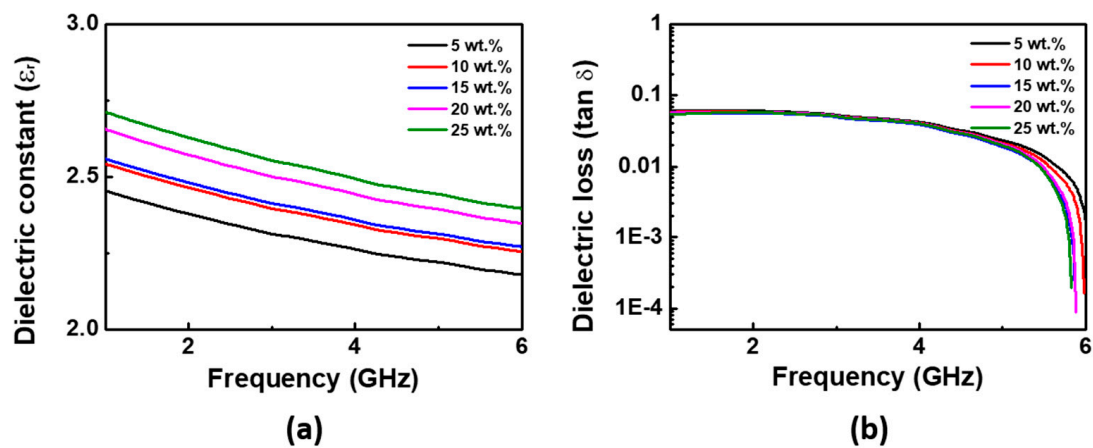


**Figure 6.** (a) Dielectric constant and (b) dielectric loss of the 3D-printed thin film with the PCL/HA composite filaments.

### 3.5. Bone Scaffold Printing with PCL/HA Composite Filaments

Figure 7 shows examples of a 3D-printed bone scaffold and a bone mimetic fabricated using filaments with 20 wt.% and 15 wt.% HA, respectively. Both 3D models were designed using 3D CAD software (Solidworks). In general, a scaffold should have a porous structure to allow bone formation and vascularization. Therefore, we designed the scaffold to have a pore size of 1200  $\mu\text{m}$ , a common pore size used for bone scaffolds [31,32]. The bone scaffold and bone mimetic structure had dimensions of 15 mm(L)  $\times$  15 mm(W)  $\times$  3 mm(T) and 35 mm(L)  $\times$  13 mm(W)  $\times$  8 mm(T), respectively. The 3D-printed scaffolds had a maximum error of 0.54 mm, which is an acceptable level of dimensional error for scaffold fabrication. It is noted that a solid structure with the same dimensions exhibits a maximum error of 0.25 mm. Thus, the filaments developed in this work can be used to make more complex structures. In addition, since the mechanical properties of bones vary with age, size, and structure, the required mechanical properties of bone scaffolds are also expected to differ slightly from one application to the next [33]. In response to this, PCL/HA filaments can be used to provide the required mechanical properties by adjusting the composition and level of porosity. The PCL/HA composite filaments can also be useful in fabricating bone mimetic testbeds and artificial bones.

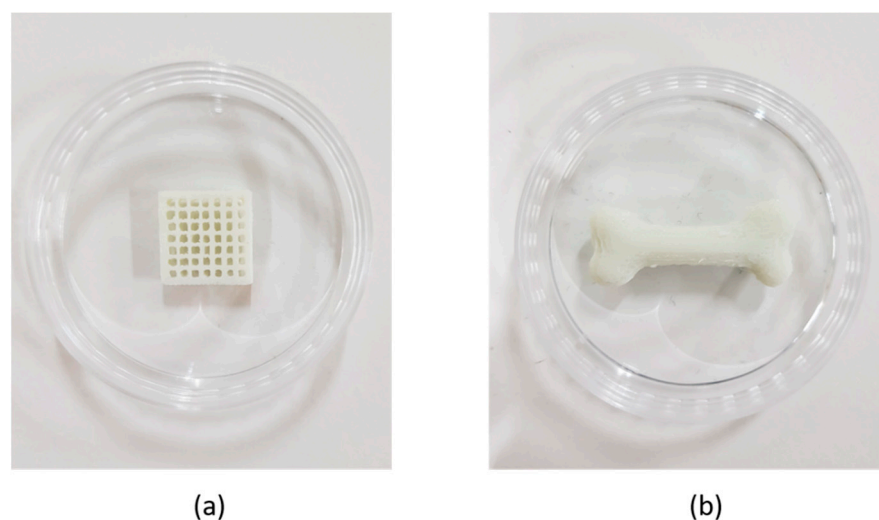


**Figure 7.** (a) 3D-printed bone scaffold and (b) bone mimetic structure.

## 4. Conclusions

In summary, we fabricated PCL/HA composite filaments with HA contents of 5, 10, 15, 20 and 25 wt.%, and used them to print bone scaffolds and bone mimetic structures

using a general FDM-type 3D printer. The morphologies and compositions of the PCL/HA composite filaments were investigated by means of SEM and XRD analysis, and a uniform filament structure and composition was confirmed. In addition, the mechanical properties of the filaments, and those of the specimens written with the fabricated filaments, were examined. We also measured their dielectric properties in the GHz range, to assess the composites' potential use as a bone-mimicking testbed for the evaluation of bone-graft-type radio devices.

**Author Contributions:** Conceptualization, J.N. and S.Y.K.; validation, C.G.K., K.S.H. and S.L.; formal analysis, K.S.H.; investigation, M.C.K.; writing—original draft preparation, C.G.K. and K.S.H.; writing—review and editing, J.N. and S.Y.K.; supervision, J.N.; funding acquisition, J.N. All authors have read and agreed to the published version of the manuscript.

**Funding:** This research was supported by the research fund of Chungnam National University.

**Institutional Review Board Statement:** Not applicable.

**Informed Consent Statement:** Not applicable.

**Data Availability Statement:** Data is contained within the article.

**Conflicts of Interest:** The authors declare no conflict of interest.

## References

1. Ngo, T.D.; Kashani, A.; Imbalzano, G.; Nguyen, K.T.Q.; Hui, D. Additive manufacturing (3D printing): A review of materials, methods, applications and challenges. *Compos. Part B Eng.* **2018**, *143*, 172–196. [[CrossRef](#)]
2. Sarvankar, S.G.; Yewale, S.N. Additive Manufacturing in Automobile Industry. *Int. J. Res. Aeronaut. Mech. Eng.* **2019**, *7*, 1–10.
3. Espera, A.H.; Dizon, J.R.C.; Chen, Q.; Advincula, R.C. 3D-printing and advanced manufacturing for electronics. *Prog. Addit. Manuf.* **2019**, *4*, 245–267. [[CrossRef](#)]
4. Tappa, K.; Jammalamadaka, U. Novel Biomaterials Used in Medical 3D Printing Techniques. *J. Funct. Biomater.* **2018**, *9*, 17. [[CrossRef](#)]
5. Chia, H.N.; Wu, B.M. Recent advances in 3D printing of biomaterials. *J. Biol. Eng.* **2015**, *9*, 4. [[CrossRef](#)]
6. Bandyopadhyay, A.; Bose, S.; Das, S. 3D printing of biomaterials. *MRS Bull.* **2015**, *40*, 108–115. [[CrossRef](#)]
7. Guvendiren, M.; Molde, J.; Soares, R.M.; Kohn, J. Designing Biomaterials for 3D Printing. *ACS Biomater. Sci. Eng.* **2016**, *2*, 1679–1693. [[CrossRef](#)] [[PubMed](#)]
8. Jammalamadaka, U.; Tappa, K. Recent Advances in Biomaterials for 3D Printing and Tissue Engineering. *J. Funct. Biomater.* **2018**, *9*, 22. [[CrossRef](#)]
9. Porter, J.R.; Ruckh, T.T.; Papat, K.C. Bone tissue engineering: A review in bone biomimetics and drug delivery strategies. *Biotechnol. Prog.* **2009**, *25*, 1539–1560. [[CrossRef](#)]
10. Cheung, H.-Y.; Lau, K.-T.; Lu, T.-P.; Hui, D. A critical review on polymer-based bio-engineered materials for scaffold development. *Compos. Part B Eng.* **2007**, *38*, 291–300. [[CrossRef](#)]
11. Gomez-Lizarraga, K.K.; Flores-Morales, C.; Del Prado-Audelo, M.L.; Alvarez-Perez, M.A.; Pina-Barba, M.C.; Escobedo, C. Polycaprolactone- and polycaprolactone/ceramic-based 3D-bioprinted porous scaffolds for bone regeneration: A comparative study. *Mater. Sci. Eng. C Mater. Biol. Appl.* **2017**, *79*, 326–335. [[CrossRef](#)]
12. Szczes, A.; Holysz, L.; Chibowski, E. Synthesis of hydroxyapatite for biomedical applications. *Adv. Colloid. Interface Sci.* **2017**, *249*, 321–330. [[CrossRef](#)]
13. Rezaei, A.; Mohammadi, M.R. In vitro study of hydroxyapatite/polycaprolactone (HA/PCL) nanocomposite synthesized by an in situ sol-gel process. *Mater. Sci. Eng. C Mater. Biol. Appl.* **2013**, *33*, 390–396. [[CrossRef](#)] [[PubMed](#)]
14. Labet, M.; Thielemans, W. Synthesis of polycaprolactone: A review. *Chem. Soc. Rev.* **2009**, *38*, 3484–3504. [[CrossRef](#)] [[PubMed](#)]
15. Totaro, A.; Salerno, A.; Imparato, G.; Domingo, C.; Urciuolo, F.; Netti, P.A. PCL-HA microscaffolds for in vitro modular bone tissue engineering. *J. Tissue Eng. Regen. Med.* **2017**, *11*, 1865–1875. [[CrossRef](#)]
16. Park, S.A.; Lee, S.H.; Kim, W.D. Fabrication of porous polycaprolactone/hydroxyapatite (PCL/HA) blend scaffolds using a 3D plotting system for bone tissue engineering. *Bioprocess Biosyst. Eng.* **2011**, *34*, 505–513. [[CrossRef](#)] [[PubMed](#)]
17. Shor, L.; Guceri, S.; Wen, X.; Gandhi, M.; Sun, W. Fabrication of three-dimensional polycaprolactone/hydroxyapatite tissue scaffolds and osteoblast-scaffold interactions in vitro. *Biomaterials* **2007**, *28*, 5291–5297. [[CrossRef](#)]
18. Zimmerling, A.; Yazdanpanah, Z.; Cooper, D.M.L.; Johnston, J.D.; Chen, X. 3D printing PCL/nHA bone scaffolds: Exploring the influence of material synthesis techniques. *Biomater. Res.* **2021**, *25*, 3. [[CrossRef](#)]
19. Ma, J.; Lin, L.; Zuo, Y.; Zou, Q.; Ren, X.; Li, J.; Li, Y. Modification of 3D printed PCL scaffolds by PVAc and HA to enhance cytocompatibility and osteogenesis. *RSC Adv.* **2019**, *9*, 5338–5346. [[CrossRef](#)]
20. Jiao, Z.; Luo, B.; Xiang, S.; Ma, H.; Yu, Y.; Yang, W. 3D printing of HA / PCL composite tissue engineering scaffolds. *Adv. Ind. Eng. Polym. Res.* **2019**, *2*, 196–202. [[CrossRef](#)]

21. Li, Y.; Yu, Z.; Ai, F.; Wu, C.; Zhou, K.; Cao, C.; Li, W. Characterization and evaluation of polycaprolactone/hydroxyapatite composite scaffolds with extra surface morphology by cryogenic printing for bone tissue engineering. *Mater. Des.* **2021**, *205*. [[CrossRef](#)]
22. Kim, M.H.; Yun, C.; Chalisserry, E.P.; Lee, Y.W.; Kang, H.W.; Park, S.-H.; Jung, W.-K.; Oh, J.; Nam, S.Y. Quantitative analysis of the role of nanohydroxyapatite (nHA) on 3D-printed PCL/nHA composite scaffolds. *Mater. Lett.* **2018**, *220*, 112–115. [[CrossRef](#)]
23. Qu, X.; Xia, P.; He, J.; Li, D. Microscale electrohydrodynamic printing of biomimetic PCL/nHA composite scaffolds for bone tissue engineering. *Mater. Lett.* **2016**, *185*, 554–557. [[CrossRef](#)]
24. Liu, D.; Nie, W.; Li, D.; Wang, W.; Zheng, L.; Zhang, J.; Zhang, J.; Peng, C.; Mo, X.; He, C. 3D printed PCL/SrHA scaffold for enhanced bone regeneration. *Chem. Eng. J.* **2019**, *362*, 269–279. [[CrossRef](#)]
25. Goncalves, E.M.; Oliveira, F.J.; Silva, R.F.; Neto, M.A.; Fernandes, M.H.; Amaral, M.; Vallet-Regi, M.; Vila, M. Three-dimensional printed PCL-hydroxyapatite scaffolds filled with CNTs for bone cell growth stimulation. *J. Biomed. Mater. Res. B Appl. Biomater.* **2016**, *104*, 1210–1219. [[CrossRef](#)] [[PubMed](#)]
26. Tian, L.; Zhang, Z.; Tian, B.; Zhang, X.; Wang, N. Study on antibacterial properties and cytocompatibility of EPL coated 3D printed PCL/HA composite scaffolds. *RSC Adv.* **2020**, *10*, 4805–4816. [[CrossRef](#)]
27. Park, S.; Kim, J.E.; Han, J.; Jeong, S.; Lim, J.W.; Lee, M.C.; Son, H.; Kim, H.B.; Choung, Y.H.; Seonwoo, H.; et al. 3D-Printed Poly(epsilon-Caprolactone)/Hydroxyapatite Scaffolds Modified with Alkaline Hydrolysis Enhance Osteogenesis In Vitro. *Polymers (Basel)* **2021**, *13*, 257. [[CrossRef](#)] [[PubMed](#)]
28. Borjigin, M.; Eskridge, C.; Niamat, R.; Strouse, B.; Bialk, P.; Kmiec, E.B. Electrospun fiber membranes enable proliferation of genetically modified cells. *Int. J. Nanomed.* **2013**, *8*, 855–864.
29. Schwerdt, H.N.; Miranda, F.A.; Chae, J. A Fully Passive Wireless Backscattering Neurorecording Microsystem Embedded in Dispersive Human-Head Phantom Medium. *IEEE Electron. Device Lett.* **2012**, *33*, 908–910. [[CrossRef](#)]
30. Rana, B.; Shim, J.-Y.; Chung, J.-Y. An Implantable Antenna With Broadside Radiation for a Brain–Machine Interface. *IEEE Sens. J.* **2019**, *19*, 9200–9205. [[CrossRef](#)]
31. Murphy, C.M.; O'Brien, F.J. Understanding the effect of mean pore size on cell activity in collagen-glycosaminoglycan scaffolds. *Cell Adhes. Migr.* **2010**, *4*, 377–381. [[CrossRef](#)] [[PubMed](#)]
32. Williams, J.M.; Adewunmi, A.; Schek, R.M.; Flanagan, C.L.; Krebsbach, P.H.; Feinberg, S.E.; Hollister, S.J.; Das, S. Bone tissue engineering using polycaprolactone scaffolds fabricated via selective laser sintering. *Biomaterials* **2005**, *26*, 4817–4827. [[CrossRef](#)] [[PubMed](#)]
33. Karipinski, R.; Jaworski, L.; Czubacka, P. The structural and mechanical properties of the bone. *J. Technol.* **2017**, *3*, 43–50.